iScience

Article

Multiple trajectories of proprioceptive drift in the mirror box illusion

Graphical abstract

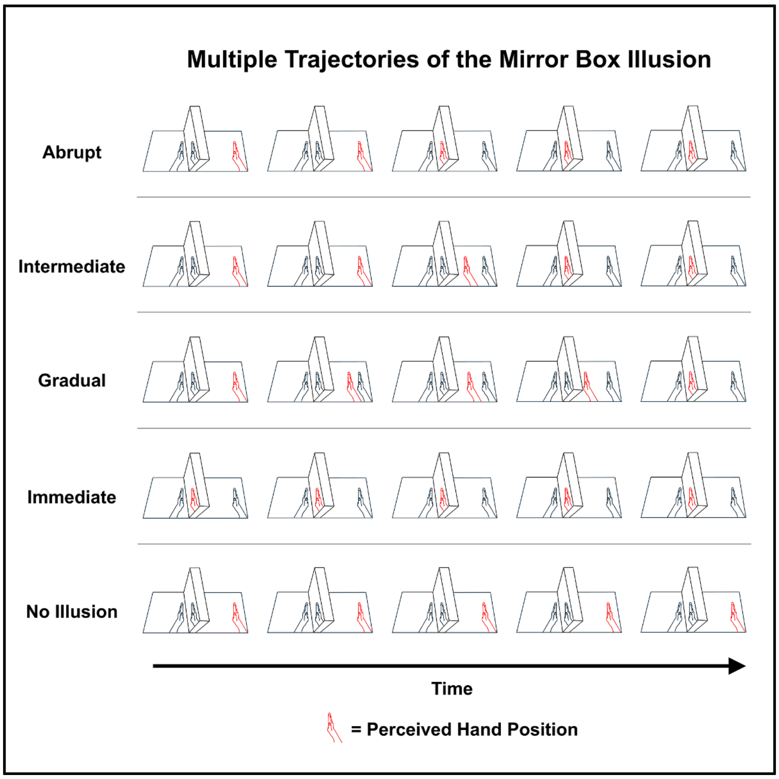

Authors

Grant T. Fairchild, Yuqi Liu, Jared Medina

Correspondence

grant.t.fairchild@gmail.com

In brief

Sensory neuroscience; Cognitive neuroscience

Highlights

- Proprioceptive drift in the mirror box illusion follows several distinct trajectories
- Visual-proprioceptive congruence modulates the incidence of these trajectories
- We observe individual variation in the distributions of these trajectories
- Variation in causal inference algorithms is a possible explanation for these patterns

Fairchild et al., 2026, iScience *29*, 116433
September 18, 2026
https://doi.org/10.1016/j.isci.2026.116433

CellPress

Article

Multiple trajectories of proprioceptive drift in the mirror box illusion

Grant T. Fairchild,[1,4,*] Yuqi Liu,[2,3] and Jared Medina[1,3]
[1]Psychology Department, Emory University, Atlanta, GA, USA
[2]Global Institute of Future Technology, Shanghai Jiao Tong University, Shanghai, China
[3]Psychology Department, The University of Delaware, Newark, DE, USA
[4]Lead contact
*Correspondence: grant.t.fairchild@gmail.com
https://doi.org/10.1016/j.isci.2026.116433

SUMMARY

The mirror box illusion creates a visual-proprioceptive conflict in which an observer's hidden hand feels like it occupies the position of their other hand's viewed reflection. We used this illusion to explore the temporal dynamics of multisensory conflict resolution, recording perceived hand position repeatedly while manipulating visual-proprioceptive congruence across four experiments within a neurotypical population (*N* = 181). Conditions with greater visual-proprioceptive congruence strengthened the illusion. Surprisingly, however, we found that the illusion follows multiple trajectories: abrupt shifts, gradual drifts, immediate onset, or no illusion at all. These trajectories are unevenly distributed across individuals, suggesting differences in observers' experience of this illusion. We advance a possible explanation in which these different trajectories could be produced by three algorithmically distinct causal inference mechanisms. By tracing the perceptual time course of individual trials, we find heterogeneity which may offer insights into the mechanisms underlying this multisensory illusion.

INTRODUCTION

Bodily illusions serve as essential tools for investigating multisensory integration between vision, touch, and proprioception (the sense of body position and orientation). By creating contexts where signals from these senses conflict with each other, illusions such as the rubber hand illusion[1] and the mirror box illusion[2,3] reveal insights into the brain's mechanisms for adjudicating evidence among competing sensory sources. Much of the work using bodily illusions assesses multisensory integration at a single endpoint, typically after a period of illusion induction. In contrast, fewer studies have focused on the temporal dynamics of multisensory integration as an unfolding process.

Previous studies of the temporal dynamics of integration between vision and somatosensation have used the rubber hand illusion, which produces a feeling of ownership over a rubber hand stroked synchronously with the observer's hidden hand.[4–7] This percept of body ownership is often accompanied by proprioceptive drift, the feeling that the position of the observer's hand is somewhere between its veridical, proprioceptively perceived location and the visually perceived location of the rubber hand. Prior work has suggested that both changes in perception of body ownership[5] and proprioceptive drift[7] occur relatively rapidly during early stages of illusion induction before plateauing or slowing. Examination of the illusion's temporal evolution[7] produced valuable insights about how the illusion is made or broken, and about how the experience of illusory body ownership may be separable from that of proprioceptive drift.[8,9] However, previous studies using the rubber hand illusion have focused only on averaged time course data across trials and across subjects, overlooking potential variability in the progression of the illusion. Additionally, while body ownership in the rubber hand illusion is frequently compelling, proprioceptive drift tends to be modest, perhaps because the incomplete verisimilitude and static nature of the rubber hand limits attribution of visual and proprioceptive signals to a common source.

By contrast, the mirror box illusion tends to elicit stronger proprioceptive drift (in the range of 20%–65% of veridical distance, compared to 5%–25% for the rubber hand illusion), with visual input more decisively overriding proprioceptive signals of hand position.[2,3,10–12] In the mirror box illusion, one hand is hidden behind a mirror while the other hand faces the mirror's surface. Because the reflection of the visible hand matches the chirality of the hidden hand, the reflection appears nearly identical to the hidden hand. This close visual similarity biases position estimates of the hidden hand when the hidden hand is placed further behind the mirror than the virtual position of the reflection. The closer match in visual appearance and the inclusion of motor congruence likely contribute to the greater proprioceptive drift relative to the rubber hand illusion. The mirror box illusion offers a promising paradigm for studying the trajectory of proprioceptive drift, since there is a larger extent along which that trajectory occurs.

While previous work using the rubber hand illusion[7] has shown that proprioceptive drift typically rises rapidly before reaching a gradual plateau, this average pattern may not represent the

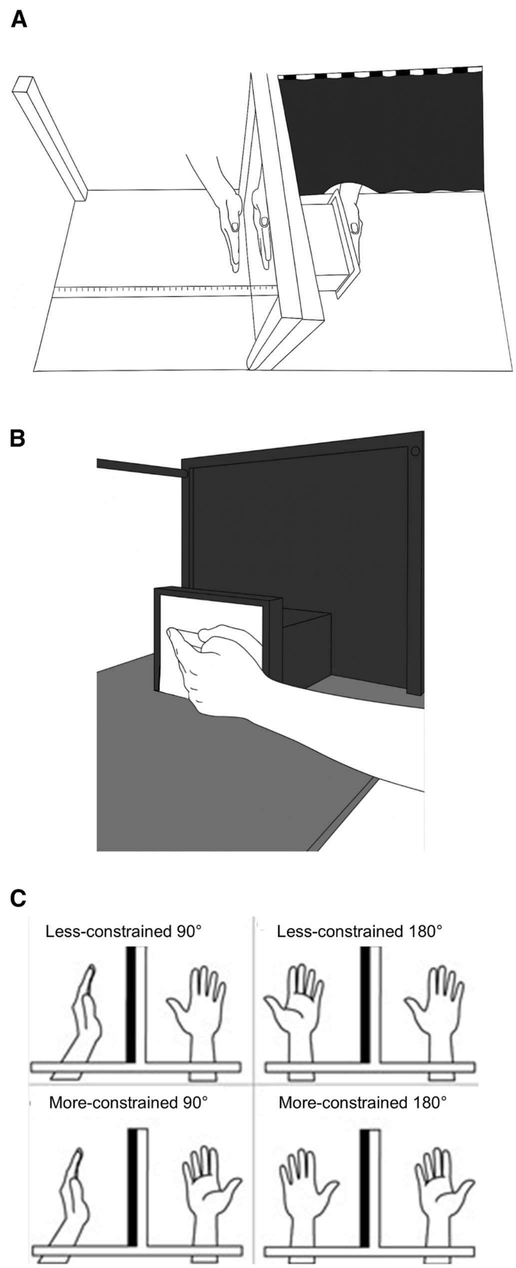

Figure 1. Mirror box illusion setup

(A) The basic setup used in the experiments.

(B) A small mirror was placed at a distance from the main mirror to serve as a surface for the hidden hand to tap against.

(C) The combinations of hand postures used in Experiment 4. The hands were offset by either 90° or 180°. Based on the positions of the two hands, rotating the left hand to match the position of the reflection hand would require either a more or less biomechanically difficult rotational movement (C. reproduced with permission from Liu & Medina, 2017).

trajectory of any individual trial. A smooth, group- and trial-averaged curve could result from averaging across heterogeneous trajectories, masking the distinct dynamics present in individual trials. Collapsing across participants also risks obscuring meaningful individual differences in the temporal unfolding of multisensory integration, the possibility of which is suggested by previous work showing age-related differences in proprioceptive drift.[13]

In the present study, we used the mirror box illusion to study the temporal progression of visual-proprioceptive integration. Participants made repeated judgments of their hidden hand's position across four experiments manipulating different aspects of visual-somatomotor congruence. We tested the effects of judgment frequency, tapping frequency, and scalar and angular disparities between the hidden hand and its reflection. In all experiments, examination of individual trials revealed qualitatively distinct trajectories of proprioceptive drift not reported in rubber-hand studies examining only the average proprioceptive drift across trials. These trajectories included trials featuring abrupt transitions in perceived hand position, trials featuring gradual shifts, trials where the illusion occurred immediately, and trials where the illusion failed to occur altogether. The tendency to experience the illusion along one trajectory type or another appeared to vary across individual observers. Intriguingly, the different trajectories closely match the predictions of different models for the implementation of multisensory causal inference. Our findings suggest surprising diversity in the temporal mechanisms for multisensory integration.

RESULTS

Our four experiments measured the time course of proprioceptive drift in the mirror box illusion (Figures 1A and 1B) while manipulating different experimental factors: Experiments 1–3 tested for effects of congruence in motor cues between the hidden and reflection hands by comparing synchronous with asynchronous tapping. Experiment 1 also tested for effects of response frequency by comparing trials where hand position was judged every 5 s with trials where hand position was judged only after 45 s. Experiment 2 tested for effects of spatial disparity between the hidden and reflection hand by comparing a 15 cm disparity with a 30 cm disparity. Experiment 3 tested for effects of cue frequency by comparing tapping movements executed at 120 BPM, tapping movements executed at 60 BPM, and trials with no tapping at all. Experiment 4 tested for effects of angular disparity between the hidden and reflection hand by comparing a 90° disparity with a 180° disparity. This experiment also tested for an effect of biomechanical constraints by comparing trials where the movement required to align the hidden and reflection hand was a biomechanically convenient movement with trials where such a movement would be biomechanically inconvenient (Figure 1C).

Conditions favoring a common cause between visual and proprioceptive signals increase proprioceptive drift

To visualize differences in the trajectory of proprioceptive drift between the different experimental conditions, we plotted the distance between the hidden hand and perceived hand position, averaged across all trials and subjects within each condition (shown in Figure 2A for Experiment 1 and in Figure S1 for Experiments 2–4). Consistent with previous studies (e.g., Medina et al., 2015), proprioceptive drift was higher in Experiment 1 during

CellPress
OPEN ACCESS

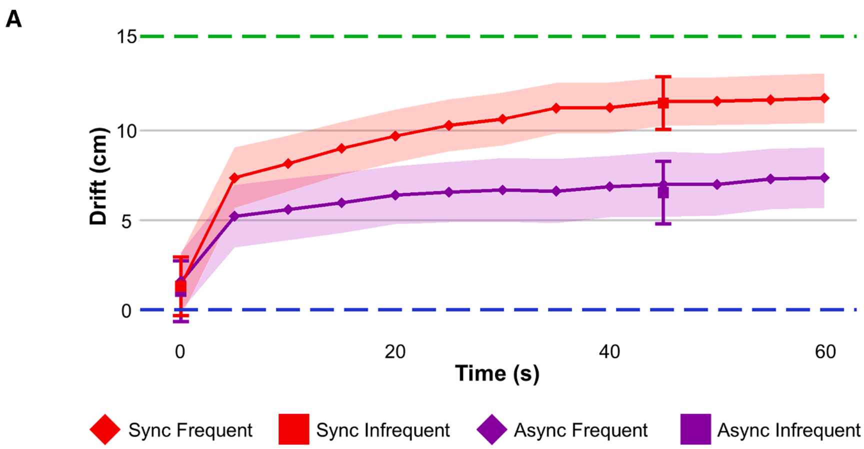

Figure 2. The time course of proprioceptive drift in individual trials follows heterogeneous trajectories that are not captured by the average across trials

(A) Average trajectories of perceived hand position relative to the veridical position of the hidden hand (i.e., proprioceptive drift) for Experiment 1. The blue dashed line indicates the veridical position of the hidden hand, while the green dashed line indicates the visual position of the reflection hand. Shading represents 95% confidence intervals for the frequent report condition, while error bars represent 95% confidence intervals for the infrequent report condition.

(B) Example trials belonging to each of the five observed categories of illusion trajectory.

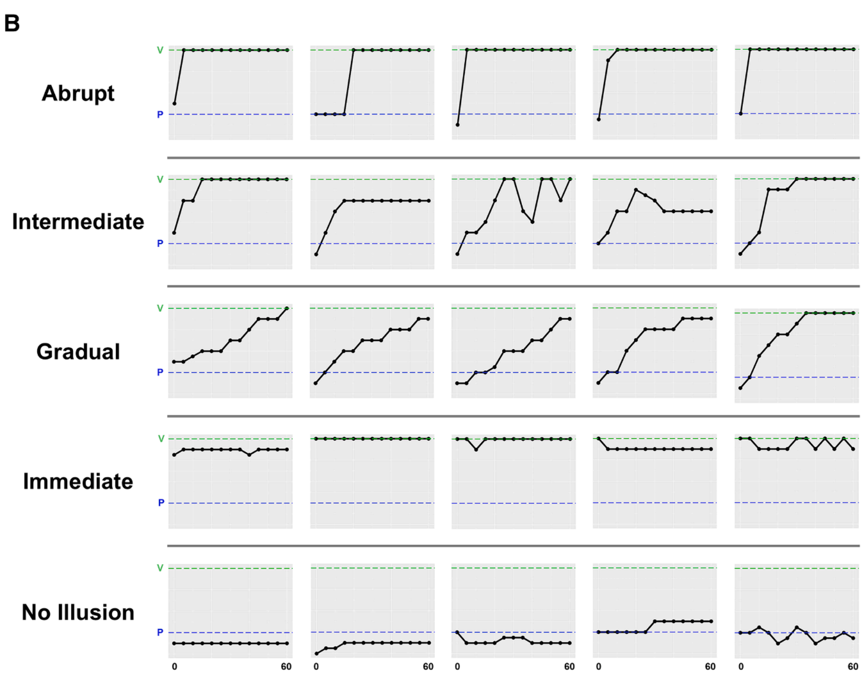

angular distance (F = 40.71, $p < 0.001$) were lower, but we observed no interaction effect (F = 1.55, $p = 0.218$). Overall, these results confirm that the illusion is strengthened by factors favoring a common cause between visual and proprioceptive signals, such as synchronous movements, minimal scalar and angular distances between the hidden hand and its mirror counterpart, and biomechanically plausible movement paths separating the two.

synchronous tapping than during asynchronous tapping (F = 45.00, $p < 0.001$). However, the two-way ANOVA revealed no effect on illusion strength for frequency of report (F = 0.58, $p = 0.449$), nor was there an interaction between synchrony and report frequency (F = 0.70, $p = 0.407$). In Experiment 2, a main effect of synchrony (F = 19.76, $p = 0.002$) replicated the results of Experiment 1, while a main effect of distance (F = 8.28, $p < 0.001$) showed that the illusion is weaker when the distance between the proprioceptive and visual estimates of hand position is larger. There was no interaction between synchrony and distance (F = 0.86, $p = 0.363$). In Experiment 3, synchronous tapping once again elicited greater proprioceptive drift than asynchronous tapping (t = 4.24, df = 37, one-tailed $p < 0.001$), but there was no effect of tapping speed (t = 0.27, df = 37, two-tailed $p = 0.785$). In Experiment 4, we observed greater proprioceptive drift when biomechanical constraint (F = 13.80, $p < 0.001$) and

Individual trials follow distinct illusion trajectories

Because the gradually sloping trajectories of Figure 2A are averaged across many subjects and trials, these averages may mask variability in the illusion trajectories of individual trials. Indeed, examination of individual trials revealed considerable variability in the shape of the trajectories. These trajectories could each be categorized into one of five different types, as seen in Figure 2B. Some trials exhibited a strikingly abrupt shift (Figure 2B, top row), typically early in the trial, in which the estimate of the hidden hand's position suddenly shifted much closer to the position of the reflection hand. Other trials showed a much more gradual drift (Figure 2B, middle row), in which the estimates slowly approached the position of the reflection hand over the course of the trial. A smaller number of intermediate trials (Figure 2B, second row) exhibited a transition in between these two extremes. In yet other trials, the illusion was experienced immediately (Figure 2B, fourth row), as soon as the observer opened their eyes and gazed into the mirror. Finally, for some trials, there was no appreciable experience of the illusion at all (Figure 2B, fifth row), with estimates of hidden hand position staying near its veridical location throughout the entire trial. We categorized each trial as belonging to one of these trajectory types based on the total extent of proprioceptive drift during the trial and the proportion of that drift that accumulated during the largest single "step" between successive position judgments (see trajectory categorization in STAR Methods). A *k*-nearest neighbors analysis showed that these trajectory categories could be correctly classified based on the underlying time series of position judgments at rates between 73% and 85% for each of Experiments 1–4. Permutation testing showed that all of these classification rates were significantly greater than chance (all *p*s < 0.001), confirming the construct validity of our trajectory categories. The distribution of trials across the five trajectory types for each condition of the four experiments is shown in Figure S2. A chi-squared test of homogeneity showed that these distributions differed across experiments ($\chi 2 = 400.6$, $p < 0.001$), and follow-up pairwise tests showed that the distributions for each pair of experiments also differed (all $p < 0.001$). The different conditions tested in each experiment may encourage different trajectory types to appear more or less frequently, though it is worth noting that all trajectory types appeared in all experiments.

Factors increasing proprioceptive drift also favor abrupt more than gradual illusion qualia

Given the finding that the mirror box illusion proceeds along different trajectories, we investigated what factors may determine whether a trial will be experienced according to one trajectory vs. another. To assess the effects of each experimental condition on the likelihood that the illusion would be experienced along each of the five trajectory types, we used binomial generalized linear mixed models (Table S1). Most notably, we found that Abrupt trials were more likely when bimanual movement was synchronous (Exp. 1, 2, and 3), when the scalar (Exp. 2) and angular (Exp. 4) distance between the visual and proprioceptive signals of hand position was lower, and when tapping rate was faster (Exp. 3). In contrast, trials without any illusion were more likely when bimanual movement was asynchronous (Exp. 1, 2, and 3), when the scalar (Exp. 2) and angular distance (Exp. 4) between the visual and proprioceptive signals of hand position was higher, and when biomechanical constraint was higher (Exp. 4). In other words, while abrupt illusion experience was favored by many of the same factors promoting proprioceptive drift, opposite factors increased the likelihood that no illusion would be experienced. Gradual trials appeared to follow an altogether different pattern than abrupt trials: Gradual trials were promoted by greater rather than lower angular distance (Exp. 4) and were also favored by lower biomechanical constraint (Exp. 4), unlike Abrupt trials. Whereas synchrony produced more Abrupt trials in every experiment where it was manipulated, this was the case for Gradual trials only in Experiment 2. Unlike with Abrupt trials, faster tapping rate did not promote Gradual trials. The divergence in experimental manipulations affecting the frequency of Abrupt vs. Gradual trials may suggest different mechanisms underlying these alternate trajectories of illusion experience.

In a secondary analysis, we used generalized linear mixed models to assess the effects of the experimental manipulations on trajectory abruptness vs. gradualness when the degree of abruptness was treated as a continuous measure rather than as a categorical outcome. As a continuous measure of abruptness, we used the standard deviation of "step" sizes between successive position judgments (ignoring trials where the illusion occurred immediately or not at all). A trial where all the proprioceptive drift accumulated during a single step would be highly abrupt and would have a large standard deviation, whereas a trial where the proprioceptive drift accumulated across many similarly sized incremental steps would be highly gradual and would have a small standard deviation. By this measure, trials were significantly more abrupt when movement was synchronous ($t = 2.67$, $p = 0.009$) in Experiment 1, when scalar distance was lower ($t = -2.13$, $p = 0.036$) in Experiment 2, when movement was synchronous ($t = 4.61$, $p < 0.001$) and when tapping was faster ($t = 2.47$, $p = 0.014$) in Experiment 3, and when angular distance was lower ($t = 5.12$, $p < 0.001$) in Experiment 4. We did not observe significant effects for synchrony ($t = -0.47$, $p = 0.637$) in Experiment 2 or for biomechanical constraint ($t = -0.99$, $p = 0.323$) in Experiment 4. With the exception of synchrony in Experiment 2, these results match those of the preceding analysis treating Abrupt trials as a categorical outcome.

Because the same factors that promote greater proprioceptive drift also increase the likelihood that the illusion will be experienced abruptly, it may be that the illusion is experienced more strongly when it is experienced more abruptly. To test this possibility, we compared proprioceptive drift in Abrupt trials with proprioceptive drift in Gradual trials (i.e., the trials where the illusion experience was least abrupt). Abrupt trials did have significantly greater proprioceptive drift than Gradual trials in Experiment 1 ($t[36.8] = -3.64$, $p < 0.001$), Experiment 3 ($t[169.9] = -4.42$, $p < 0.001$), and Experiment 4 ($t[153.7] = -2.15$, $p = 0.033$), but not in Experiment 2 ($t[57.3] = -0.61025$, $p = 0.544$).

Participants show individual differences in illusion trajectories

We observed that many participants tended to experience the illusion predominantly along one trajectory or another: For instance, some participants experienced the illusion abruptly in every trial, while others never experienced the illusion in any trial (Figure S3). To determine whether these individual differences were significant, we ran 10,000 Monte Carlo simulations in which illusion trajectories were assigned to simulated trials and subjects in proportion to the frequency of each trajectory type in the full dataset (Table S2). The trajectories were more evenly distributed across participants in the simulations than in the experimental data (all $p < 0.01$). These results indicate that individual subjects do have significantly different profiles of tendencies to experience the distinct types of illusion trajectory. While many participants predominantly experienced one illusion trajectory more than any of the other trajectories, it is worth noting that a minority of participants showed no strong preference for one trajectory over the others. To test for individual differences using a method agnostic to trajectory category definitions, we also examined distances between trials in the 13-dimensional space described by the time series of hand position judgments, comparing distances for trial pairs within participants to distances for trial pairs between participants. For all four experiments, within-participant distances were smaller than between-participant distances (all $p < 0.001$).

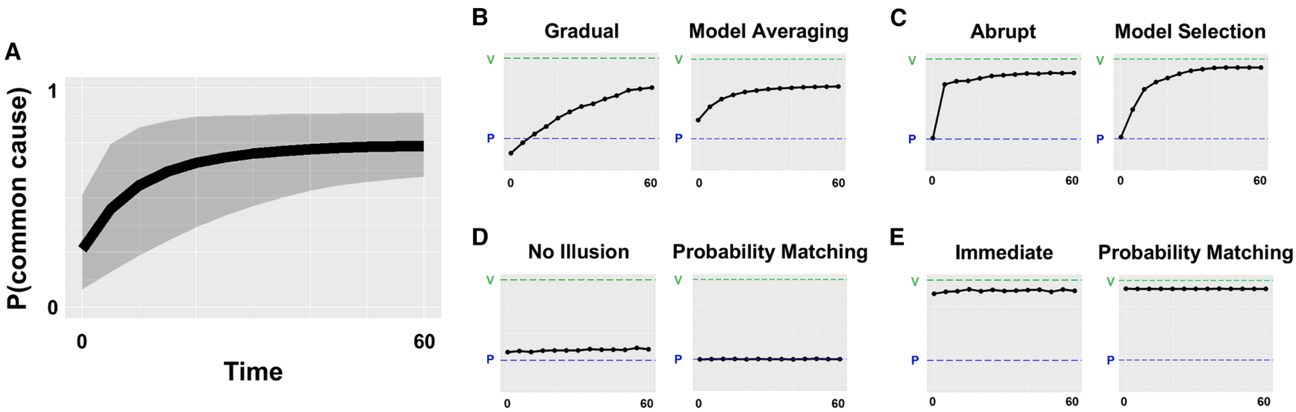

Figure 3. Different illusion trajectory types are predicted by different decision strategies for causal inference

(A) Average *p(common)* curve across 1,000 simulated trials, with shaded region corresponding to 95% confidence interval. As evidence accumulates that visual and proprioceptive signals are congruent, the probability that the two signals are caused by a common source increases.

(B–E) Average time courses of trials of different drift trajectory types in experiment 1 (left panels) are shown alongside averages of 1,000 simulated trials using different decision strategies (right panels). Gradual trials may result from a model averaging strategy (B), Abrupt trials from a model selection strategy (C), and both No Illusion (D) and Immediate (E) trials from a Probability Matching strategy.

DISCUSSION

Across four experiments, we used the mirror box illusion to investigate the temporal dynamics of proprioceptive drift. We identified multiple distinguishable trajectories for the progression of the illusion over time, including sharply abrupt and smoothly gradual patterns. Individual participants showed significant tendencies toward particular trajectory types. This variability raises important questions about the heterogeneity of the mechanisms underlying multisensory integration: What distinct processes might produce the different patterns we observed?

One possibility is that these different experiences of the illusion arise from distinct strategies for adjudicating between causal hypotheses about the sources of sensory signals. According to Bayesian causal inference frameworks for multisensory integration, when the brain receives two signals that may derive from either a single source or from separate sources, it considers both causal possibilities.[14] If the two signals originate from separate sources, accurate estimates are obtained by segregating the signals rather than integrating them. If, however, both signals are noisy estimates of the same underlying event, then a more reliable estimate can be formed by combining them, weighting each signal by its reliability.[15–17] Whether to use the resulting maximum likelihood estimate thus depends on the probability that the two signals share a common cause, *p(common)*. For a given value of *p(common)*, the brain could apply different decision strategies for combining or ignoring unisensory and integrated estimates.[18]

Model averaging is the most commonly assumed and frequently successful implementation of Bayesian causal inference.[14,19–23] Under this decision strategy, both the unisensory and the integrated (maximum likelihood) estimate contribute to the overall percept, weighted by *p(¬common)* and *p(common)*, respectively. During the mirror box illusion, *p(common)* likely increases as evidence accumulates favoring the single-source hypothesis, eventually leveling off (Figure 3A). As *p(common)* rises, the perceived hand position should gradually shift from the veridical position indicated by the proprioceptive signal toward the vision-dominated maximum likelihood estimate near the position of the reflection hand. Whether *p(common)* increases linearly or nonlinearly, a system using Model Averaging would produce the smooth, progressive shifts characteristic of the Gradual trajectories we observed (Figure 3B). Trials intermediate between Abrupt and Gradual trajectories could reflect Model Averaging in cases where *p(common)* increased more quickly than in the Gradual trials.

Alternatively, the brain might employ a Model Selection strategy, choosing the most likely causal structure at each moment and relying exclusively on its associated estimate. Under this approach, the proprioceptive estimate would be used whenever *p(common)* < 0.5, while the maximum likelihood estimate would be used whenever *p(common)* > 0.5. As *p(common)* increases during a trial, this decision strategy would yield an abrupt phase transition in perceived hand position as soon as the threshold is crossed, consistent with the Abrupt trajectories in our data (Figure 3C).

Finally, the brain could choose a single causal structure for each trial with frequency proportional to the probability of that causal structure at trial onset. Although such a Probability Matching strategy may be counterintuitive, some previous studies have found this approach a better model for causal inference than competing decision strategies.[18,24,25] Under this strategy, the proprioceptive estimate would be selected with frequency equal to *p(¬common)*, and the maximum likelihood estimate would be selected with frequency equal to *p(common)*, producing trajectories similar to the No Illusion (Figure 3D) and Immediate (Figure 3E) trajectories we observed. The greater number of No Illusion than Immediate trials across experiments aligns with the expectation that *p(common)* begins low at trial onset before rising during illusion induction. One could imagine a Probability Matching strategy that evaluated *p(common)* continuously rather than at trial onset, which would produce a sawtooth trajectory alternating between the proprioceptive estimate and the maximum likelihood estimate (Figure S4). However, such trajectories were not typical in our datasets, and such a strategy would seem to produce impractically volatile, flickering percepts ill-suited for stable perception of an observer's body and surroundings.

While use of different decision strategies could produce the different patterns of proprioceptive drift we observed, crossmodal recalibration could also contribute to these patterns. Indeed, proprioceptive recalibration has previously been reported in the mirror box illusion.[3] Whereas multisensory integration shifts perceived hand position to a point intermediate between the visual and proprioceptive signals, recalibration could shift the proprioceptive signal itself toward the visual signal over time. Sensory recalibration is typically considered a cumulative process resulting from consistent exposure to discrepant multisensory signals.[26] In our trials, a proprioceptive signal that is gradually shifting toward the visual signal through recalibration could produce a shift in the multisensory hand estimate similar to what we observed in our Gradual trials. However, our ability to draw conclusions about the role of recalibration is limited by the fact that we only ever measured perceived hand position in the presence of the visual signal (the mirror hand), whereas recalibration would ideally be measured in the absence of this signal to isolate the effects of multisensory integration on overall hand estimates combining visual and proprioceptive signals from the effects of recalibration on the proprioceptive signal itself.[27,28] Future work could disentangle any effects of crossmodal recalibration from the effects of different decision strategies for multisensory integration.

By identifying the heterogeneity of illusory experience across individual trials, the present findings advance on previous studies of the temporal dynamics of multisensory integration.[4–7] Our results diverge from some of this previous research[7] in finding no effect of report frequency on proprioceptive drift. Rohde et al., 2011 found an interaction effect between report frequency and tactile synchrony in the rubber hand illusion, such that more frequent reports made proprioceptive drift more comparable between synchronous and asynchronous stroking. However, in that study, stroking of the rubber and real hand was interrupted whenever observers reported perceived hand position, whereas in our experiment, tapping of the visible and hidden hands was not interrupted when observers reported perceived hand position. This suggests that report frequency only affects proprioceptive drift when reports interrupt cues to the likelihood of a common cause for visual and somatosensory signals.

While decision strategies are sometimes treated as competing models for causal inference, our findings raise the possibility that the brain may flexibly employ multiple strategies across individuals, or even within the same individual at different times. Earlier research on audiovisual integration found that different observers' responses were best modeled by different decision strategies.[18] Intriguingly, the proportions of observers in that study favoring model averaging, model selection, and probability matching roughly match the proportions of our observers who preferentially experienced the Gradual, Abrupt, and Immediate/No Illusion trajectories, respectively. Although this correspondence is speculative, it raises the possibility that individuals may have stable, trait-like tendencies toward particular implementations of causal inference. Testing whether these tendencies persist over time would require further study, as our single-session design represents a key limitation, restricting our ability to draw conclusions about the stability of individual differences (though see[29] for evidence of stable individual differences in the related rubber hand illusion). Another limitation concerns generalizability: these individual differences, and our broader results, may not extend to older populations, given known age-related changes in visual-proprioceptive perception of body position.[13] While our experiments suggest possible differences in the preferred mechanisms of causal inference across individuals, the fact that many observers experienced multiple trajectory types is consistent with the possibility that multiple inference mechanisms may co-exist even within a single observer's brain, recruited dynamically depending on external context or internal state.

Heterogeneity in observers' experience of the mirror box illusion evinced itself only because we examined multisensory integration as a temporally extended process rather than as a static endpoint. Whereas single endpoint measurements reveal only the outcome of multisensory conflict resolution, repeated sampling across time allows investigation of the processes leading to that outcome. By examining trajectories of proprioceptive drift in individual trials, the present study expands on previous research on the temporal evolution of visuo-somatosensory integration.[4–7] Our results highlight that otherwise hidden mechanistic diversity can be uncovered by investigation of the temporal dynamics of illusion qualia on a trial-wise basis.

Limitations of the study

In addition to the questions our study design is not suited to address, such as whether the observed individual differences are stable traits or whether multisensory recalibration could contribute to the observed proprioceptive drift, several factors limit interpretation of our findings. Perhaps most critically, the definitions for the trajectory types we observed were defined *a priori*, rather than as the outcome of an unsupervised clustering or model-fitting analysis. Although a *post hoc k*-nearest neighbors analysis confirmed that these category definitions map onto underlying patterns in trajectory space, our category boundaries may not represent the best possible boundaries, or even the ideal number of categories. Although our trajectory categories are distinguishable from one another, they do exist on a spectrum, with Intermediate trials blending between Abrupt and Gradual trials. Because the illusion trajectories lie on a continuum, a different classification scheme could have instead grouped the Intermediate trials into one of the adjacent categories. Although we hypothesize distinct mechanisms, these distinct mechanisms may produce ranges of trajectories that partially overlap with each other.

Because our study was designed with the intention of comparing conditions within experiments, it is difficult to compare our results across our four experiments, which differed in their methodological details. The experiments tested different factors, used different variants of the mirror box illusion, and were collected at two different sites with two different sets of experimenters. Thus, although a chi-squared test indicated that the distributions of trajectory types differed across experiments, we are unable to confidently identify the source of those differences. One possibility is that the lack of position cues coming from the absence of surface contact in Experiment 4 could have increased proprioceptive uncertainty, and greater proprioceptive uncertainty could alter *p(common)*.[30] However, differences between the trajectory distributions of the other experiments, which all included position cues from surface contact, suggest that other factors contribute to the distributional differences between experiments. Although we cannot draw conclusions based on these differences, the similarity of other results across experiments suggests important commonalities. That the different trajectory types were observed in all experiments and that there were individual differences in all experiments indicates that the appearance of these heterogeneous trajectories is not a quirk particular to any particular illusion variant and likely has a source in multisensory processing common to all experiments.

Although we hypothesize that different decision strategies for causal inference may be the source of these different trajectory types, the current set of experiments is unable to demonstrate this definitively. Our experiments were not designed to test this possibility against other potential mechanistic explanations for the different trajectory types. Future experiments could evaluate this framework by testing its predictions, perhaps using experimental conditions designed to modulate *p(common)*, for instance by varying proprioceptive[30] or visual[31,32] reliability. Future work could also isolate the effects of multisensory integration on proprioceptive drift from potential effects of multisensory recalibration. While the present studies demonstrate consistent diversity in the qualitative experience of this multisensory illusion, the mechanisms responsible for this diversity remain an open question.

RESOURCE AVAILABILITY

Lead contact

Requests for further information and resources should be directed to and will be fulfilled by the lead contact, Grant T. Fairchild (grant.t.fairchild@gmail.com).

Materials availability

This study did not generate new unique reagents.

Data and code availability

- Experimental data have been deposited at OSF and are publicly available as of the date of publication at OSF: https://doi.org/10.17605/OSF.IO/MZK7D.
- All original code has been deposited at OSF and is publicly available as of the date of publication at OSF: https://doi.org/10.17605/OSF.IO/MZK7D.
- Any additional information required to reanalyze the data reported in this study is available from the lead contact upon request.

ACKNOWLEDGMENTS

We thank Kerri Walter, Cathy Nadar, Cara Jones, Chris Rochester, Audrey Berry, Chloe Esterly, Wayne Wang, Sarah Kaiser, Riley Dowdall, and Emma Ceklosky for assistance with data collection, and Manya Bansal for assistance with figure illustrations. This project was funded by NSF grant 1632849.

AUTHOR CONTRIBUTIONS

G.T.F.: conceptualization, data curation, formal analysis, investigation, methodology, project administration, software, validation, visualization, writing – original draft, and writing – review and editing. Y.L.: conceptualization, investigation, methodology, project administration, software, and visualization. J.M.: conceptualization, funding acquisition, methodology, project administration, resources, supervision, writing – review and editing.

DECLARATION OF INTERESTS

The authors have no competing interests to declare.

DECLARATION OF GENERATIVE AI AND AI-ASSISTED TECHNOLOGIES IN THE WRITING PROCESS

During the preparation of this work the authors used ChatGPT in order to smooth edges in the illustrations of Figure 1. After using this tool/service, the authors reviewed and edited the content as needed and take full responsibility for the content of the published article.

STAR★METHODS

Detailed methods are provided in the online version of this paper and include the following:

- KEY RESOURCES TABLE
- EXPERIMENTAL MODEL AND STUDY PARTICIPANT DETAILS
  - Sample size and characteristics
- METHOD DETAILS
  - Apparatus
  - Procedure
- QUANTIFICATION AND STATISTICAL ANALYSIS
  - Proprioceptive drift and illusion strength
  - Trajectory categorization
  - Binomial mixed models
  - Tests for individual differences
  - Decision strategy simulations
  - Subject exclusion

SUPPLEMENTAL INFORMATION

Supplemental information can be found online at https://doi.org/10.1016/j.isci.2026.116433.

Received: December 31, 2025
Revised: April 1, 2026
Accepted: June 1, 2026

REFERENCES

1. Botvinick, M., and Cohen, J. (1998). Rubber hands ‘feel’touch that eyes see. Nature *391*, 756. https://doi.org/10.1038/35784.
2. Holmes, N.P., Crozier, G., and Spence, C. (2004). When mirrors lie: “Visual capture” of arm position impairs reaching performance. Cogn. Affect. Behav. Neurosci. *4*, 193–200. https://doi.org/10.3758/CABN.4.2.193.
3. Holmes, N.P., and Spence, C. (2005). Visual bias of unseen hand position with a mirror: spatial and temporal factors. Exp. Brain Res. *166*, 489–497. https://doi.org/10.1007/s00221-005-2389-4.
4. Abdulkarim, Z., Hayatou, Z., and Ehrsson, H.H. (2021). Sustained rubber hand illusion after the end of visuotactile stimulation with a similar time course for the reduction of subjective ownership and proprioceptive drift. Exp. Brain Res. *239*, 3471–3486. https://doi.org/10.1007/s00221-021-06211-8.

5. Finotti, G., Garofalo, S., Costantini, M., and Proffitt, D.R. (2023). Temporal dynamics of the rubber hand illusion. Sci. Rep. *13*, 7526. https://doi.org/10.1038/s41598-023-33747-2.
6. Mosch, B., Fuchs, X., Tu, T., and Diers, M. (2025). Time course of the rubber hand illusion–induced analgesia. Pain Rep. *10*, e1252. https://doi.org/10.1097/PR9.0000000000001252.
7. Rohde, M., Di Luca, M., and Ernst, M.O. (2011). The rubber hand illusion: feeling of ownership and proprioceptive drift do not go hand in hand. PLoS One *6*, e21659. https://doi.org/10.1371/journal.pone.0021659.
8. Holle, H., McLatchie, N., Maurer, S., and Ward, J. (2011). Proprioceptive drift without illusions of ownership for rotated hands in the "rubber hand illusion" paradigm. Cogn. Neurosci. *2*, 171–178. https://doi.org/10.1080/17588928.2011.603828.
9. Keizer, A., Smeets, M.A.M., Postma, A., van Elburg, A., and Dijkerman, H.C. (2014). Does the experience of ownership over a rubber hand change body size perception in anorexia nervosa patients? Neuropsychologia *62*, 26–37. https://doi.org/10.1016/j.neuropsychologia.2014.07.003.
10. Costantini, M., Robinson, J., Migliorati, D., Donno, B., Ferri, F., and Northoff, G. (2016). Temporal limits on rubber hand illusion reflect individuals' temporal resolution in multisensory perception. Cognition *157*, 39–48. https://doi.org/10.1016/j.cognition.2016.08.010.
11. Medina, J., Khurana, P., and Coslett, H.B. (2015). The influence of embodiment on multisensory integration using the mirror box illusion. Conscious. Cogn. *37*, 71–82. https://doi.org/10.1016/j.concog.2015.08.011.
12. Riemer, M., Bublatzky, F., Trojan, J., and Alpers, G.W. (2015). Defensive activation during the rubber hand illusion: Ownership versus proprioceptive drift. Biol. Psychol. *109*, 86–92. https://doi.org/10.1016/j.biopsycho.2015.04.011.
13. Teramoto, W. (2022). Age-related changes in visuo-proprioceptive processing in perceived body position. Sci. Rep. *12*, 8330. https://doi.org/10.1038/s41598-022-12022-w.
14. Körding, K.P., Beierholm, U., Ma, W.J., Quartz, S., Tenenbaum, J.B., and Shams, L. (2007). Causal inference in multisensory perception. PLoS One *2*, e943. https://doi.org/10.1371/journal.pone.0000943.
15. Alais, D., and Burr, D. (2004). The ventriloquist effect results from near-optimal bimodal integration. Curr. Biol. *14*, 257–262. https://doi.org/10.1016/j.cub.2004.01.029.
16. Ernst, M.O., and Banks, M.S. (2002). Humans integrate visual and haptic information in a statistically optimal fashion. Nature *415*, 429–433. https://doi.org/10.1038/415429a.
17. Ernst, M.O., and Bülthoff, H.H. (2004). Merging the senses into a robust percept. Trends Cogn. Sci. *8*, 162–169. https://doi.org/10.1016/j.tics.2004.02.002.
18. Wozny, D.R., Beierholm, U.R., and Shams, L. (2010). Probability matching as a computational strategy used in perception. PLoS Comput. Biol. *6*, e1000871. https://doi.org/10.1371/journal.pcbi.1000871.
19. Acerbi, L., Dokka, K., Angelaki, D.E., and Ma, W.J. (2018). Bayesian comparison of explicit and implicit causal inference strategies in multisensory heading perception. PLoS Comput. Biol. *14*, e1006110. https://doi.org/10.1371/journal.pcbi.1006110.
20. Aller, M., and Noppeney, U. (2019). To integrate or not to integrate: Temporal dynamics of hierarchical Bayesian causal inference. PLoS Biol. *17*, e3000210. https://doi.org/10.1371/journal.pbio.3000210.
21. Cao, Y., Summerfield, C., Park, H., Giordano, B.L., and Kayser, C. (2019). Causal inference in the multisensory brain. Neuron *102*, 1076–1087.e8. https://doi.org/10.1016/j.neuron.2019.03.043.
22. Rohe, T., and Noppeney, U. (2015). Sensory reliability shapes perceptual inference via two mechanisms. J. Vis. *15*, 22. https://doi.org/10.1167/15.5.22.
23. Verhaar, E., Medendorp, W.P., Hunnius, S., and Stapel, J.C. (2022). Bayesian causal inference in visuotactile integration in children and adults. Dev. Sci. *25*, e13184. https://doi.org/10.1111/desc.13184.
24. Mendonça, C., Mandelli, P., and Pulkki, V. (2016). Modeling the perception of audiovisual distance: Bayesian causal inference and other models. PLoS One *11*, e0165391. https://doi.org/10.1371/journal.pone.0165391.
25. Tanaka, T. (2024). Evaluating the Bayesian causal inference model of intentional binding through computational modeling. Sci. Rep. *14*, 2979. https://doi.org/10.1038/s41598-024-53071-7.
26. Bruns, P., and Röder, B. (2023). Development and experience-dependence of multisensory spatial processing. Trends Cogn. Sci. *27*, 961–973. https://doi.org/10.1016/j.tics.2023.04.012.
27. Debats, N.B., Heuer, H., and Kayser, C. (2021). Visuo-proprioceptive integration and recalibration with multiple visual stimuli. Sci. Rep. *11*, 21640. https://doi.org/10.1038/s41598-021-00992-2.
28. Debats, N.B., Heuer, H., and Kayser, C. (2023). Different time scales of common-cause evidence shape multisensory integration, recalibration and motor adaptation. Eur. J. Neurosci. *58*, 3253–3269. https://doi.org/10.1111/ejn.16095.
29. Bekrater-Bodmann, R., Foell, J., Diers, M., and Flor, H. (2012). The perceptual and neuronal stability of the rubber hand illusion across contexts and over time. Brain Res. *1452*, 130–139. https://doi.org/10.1016/j.brainres.2012.03.001.
30. Chancel, M., and Ehrsson, H.H. (2023). Proprioceptive uncertainty promotes the rubber hand illusion. Cortex *165*, 70–85. https://doi.org/10.1016/j.cortex.2023.04.005.
31. Okumura, K., Ora, H., and Miyake, Y. (2020). Investigating the hand ownership illusion with two views merged in. Front. Robot. AI *7*, 49. https://doi.org/10.3389/frobt.2020.00049.
32. Pamplona, G., Gruaz, Q., Mauron, K., and Ionta, S. (2022). Abrupt visibility modifications affect specific subjective (not objective) aspects of body ownership. Acta Psychol. *229*, 103672. https://doi.org/10.1016/j.actpsy.2022.103672.
33. Brainard, D.H. (1997). The psychophysics toolbox. Spat. Vis. *10*, 433–436.
34. Liu, Y., and Medina, J. (2017). Influence of the body schema on multisensory integration: Evidence from the mirror box illusion. Sci. Rep. *7*, 5060. https://doi.org/10.1038/s41598-017-04797-0.

CellPress
OPEN ACCESS

STAR★METHODS

KEY RESOURCES TABLE

REAGENT or RESOURCE	SOURCE	IDENTIFIER
Deposited data		
Raw data for Experiments 1, 2, 3, and 4	OSF repository	https://doi.org/10.17605/OSF.IO/MZK7D
Software and algorithms		
MATLAB_R2024B	The Math Works, Natick, MA, USA	https://www.mathworks.com/products/matlab.html
Psychtoolbox_3.0.19	Brainard[33]	http://psychtoolbox.org/
E-Prime_3.0.3.31	Psychology Software Tools, Inc.	https://pstnet.com/products/e-prime/
RStudio_2023.09.01	Posit Software, Boston, MA, USA	https://posit.co/download/rstudio-desktop/
Runtime and analysis code for Experiments 1, 2, 3, and 4	OSF repository	https://doi.org/10.17605/OSF.IO/MZK7D

EXPERIMENTAL MODEL AND STUDY PARTICIPANT DETAILS

Sample size and characteristics

43 individuals participated in Experiment 1 (27 females, mean age: 19.2, range: 18–24), 34 in Experiment 2 (25 females, mean age: 18.8, range: 18–21), 39 in Experiment 3 (30 females, mean age: 19.3, range: 18–22), and 64 in Experiment 4 (39 females, mean age: 18.8, range: 18–26). Additional demographic data (e.g., gender identity, race, ethnicity, ancestry, or socioeconomic status) were not collected. The sample size for each experiment is similar to those used in studies of the temporal dynamics of visual-proprioceptive integration using the rubber hand illusion.[4–7] A *post-hoc* power sensitivity analysis confirmed that our samples had adequate statistical power to detect significant effects of our experimental manipulations on the frequency of the different illusion trajectory categories (Table S3). Participants provided verbal assent as approved by the Institutional Review Boards of The University of Delaware (1605549-1) and Emory University (2024P007775). Participants were undergraduates who received course credit as compensation for their time.

METHOD DETAILS

Apparatus

The illusion was induced in a mirror box apparatus consisting of an 81 × 41 cm flat wooden base bisected by a one-sided 30 cm-tall acrylic mirror, with the mirror surface facing the right side of the apparatus (Figure 1A). Participants placed the right hand to the right of the mirror surface and the left hand to the left of the mirror's surface, hidden behind it. During trials, participants gazed into the mirror from the right side, such that the reflection of the right hand looked like the hidden left hand. A curtain hung from the front left side of the apparatus was draped over the participant's left arm and shoulder to occlude vision of the left limb. A ruler printed on paper was placed behind the participant's right hand. The numbers on this ruler were printed in reverse, with the lowest numbers closest to the mirror's surface, so that participants could make numerical position judgments by reading the ruler within the mirror's reflection. To prevent participants from anchoring to a single number across trials, we used four different rulers which began and ended with different numbers; these rulers were switched out between trials in a randomized, evenly distributed order.

In Experiment 1, a mirror affixed to a small box was placed 15 cm behind the surface of the primary mirror (Figure 1B). This second mirror was not viewed by the participant; instead, its purpose was to provide a surface for the left hand to tap against which would match the tactile experience of the mirror surface which the right hand was tapping against. In Experiment 2, this secondary mirror was placed either 15 cm or 12 cm behind the surface of the primary mirror. Experiment 3 required no additional equipment beyond the basic mirror box apparatus, as participants in this experiment tapped their hands against the base of the apparatus, rather than against the mirror surface. In Experiment 4, adjustable wooden frames constrained each of the participant's hands to the appropriate angle for each trial, with minimal space for wrist rotation once tightened. These frames were placed 15 cm on either side of the mirror.

Procedure

Basic procedure

At the start of each experimental session, participants were given instructions for the experiment and were positioned with their right hand 2.5 cm from the primary mirror surface and their left hand 2.5 cm from the secondary mirror surface. Hand placement locations were marked with tape on the base of the apparatus. The hands were oriented vertically, with the thumb at top and the fifth finger at bottom, resting on the base of the apparatus. Participants were instructed to maintain a symmetrical posture between the two hands and the two arms.

Participants made numerical judgments about the position of the hidden left hand with reference to the ruler viewed through the mirror's reflection. Participants made a baseline judgment at the start of each trial, and made additional judgments when cued by an auditory tone every 5 s throughout the 60-s duration of the trial, resulting in 13 total position judgments per trial. In between trials, participants were asked to shake out their hands and to close their eyes. Participants opened their eyes immediately before trial onset.

After the initial judgment of hand position, participants executed tapping movements throughout the duration of the trial. These tapping movements were set to the beat of a metronome sounding at 70 beats per minute. Tapping movements were either synchronous or asynchronous. Synchronous tapping required the index finger of each hand to tap the mirror's surface simultaneously, and to extend away from the mirror surface simultaneously. Asynchronous tapping required the index finger of one hand to tap the surface as the index finger of the other hand extended away from the surface, and vice versa. Synchronous tapping provides congruent cues between visual, proprioceptive, tactile, and motor efferent signals, while asynchronous tapping produces visual cues that are incongruent with proprioceptive, tactile, and motor efferent signals. Previous research[11] has shown that synchronous tapping strengthens the experience of the mirror box illusion, while asynchronous tapping weakens it.

Participants reported their position judgments verbally, and responses were input by the experimenter. Response input and trial order was controlled using custom MATLAB scripts (version r2024b, The Mathworks, Inc.) running Psychtoolbox[33] (version 3.0.19) and using E-Prime (version 3.0.3.31, Psychology Software Tools, Inc.).

Experiment 1

Experiment 1 followed a 2 (judgment frequency) X 2 (movement synchrony) within-subjects design. There were 3 trials per condition for a total of 12 trials per subject. Position judgments were made either frequently (every 5 s, as in the Basic Procedure) or infrequently (once at the start of the trial, and once after 45 s). Tapping movements were executed either synchronously or asynchronously, as in the Basic Procedure.

Experiment 2

Experiment 2 followed a 2 (hidden hand distance) X 2 (movement synchrony) within-subjects design. There were 3 trials per condition for a total of 12 trials per subject. The secondary mirror was placed either 15 cm or 30 cm behind the primary mirror, such that the hidden hand was either 18 cm or 33 cm behind the primary mirror. Tapping movements were executed either synchronously or asynchronously, as in the Basic Procedure.

Experiment 3

Experiment 3 followed a 2 (rate of tapping) X 2 (movement synchrony) within-subjects design, with an additional condition where no tapping movements were executed. There were 4 trials per condition for a total of 20 trials per subject. Tapping movements were executed either at a slow rate of 60 beats-per-minute or at a fast rate of 180 beats-per-minute. Tapping movements were executed either synchronously or asynchronously. Unlike in the Basic Procedure, the hands were positioned palms-down, and tapping movements were made with the index fingers against the base of the apparatus, rather than against the surfaces of the mirrors. The right index finger was positioned 4 cm away from the mirror's surface. The left index finger was positioned 34 cm behind the mirror's surface, such that it was 30 cm away from the apparent position of the reflection finger.

Experiment 4

Experiment 4 followed a 2 (angular disparity) X 2 (biomechanical constraint) within-subjects design. There were 4 trials per condition for a total of 16 trials per subject. Experiment 4 used a different variant of the mirror box illusion, first described by Liu and Medina, 2017. Whereas the other experiments featured a translational displacement between the hidden hand and the apparent location of the reflection of the visible hand, Experiment 4 featured an angular displacement between the hidden hand and the reflection. With each hand placed in wooden frames that limited deviation from the intended hand orientation, the visible right hand was oriented palm-up or palm-down, and the hidden left hand was oriented palm-up, palm-down, or thumb-up (Figure 1C). As such, the hidden hand was displaced angularly either by 90° or by 180° from the reflection hand. Depending on the position of the two hands, the rotational movement required for the hidden hand to match the reflection hand was either a less or more biomechanically constrained movement. The amount of biomechanical constraint associated with this hypothetical movement has previously been shown to modulate the strength of the illusion.[34] Instead of judging the translational position of the hidden hand, participants judged the angular position of the hidden hand. These judgments were made with reference to a chart showing 12 hand postures rotated along even intervals of 30°. Each posture was labeled with a letter, which participants would name to select the hand posture most similar to the posture they perceived their hidden hand to occupy. Throughout the duration of the trial, participants synchronously closed and opened both hands at a rate of 100 BPM.

QUANTIFICATION AND STATISTICAL ANALYSIS

All analyses were completed using R (RStudio version 2023.09.01, R version 4.4.3).

Proprioceptive drift and illusion strength

Proprioceptive drift was measured as the distance (angular distance in the case of Experiment 4) between the perceived position of the hidden hand and the actual position of the hidden hand. The maximum proprioceptive drift recorded during a trial was used as a measure of the strength of the illusion during that trial. This value was the input for the ANOVAs comparing strength of the illusion across conditions.

Trajectory categorization

The trajectory of the illusion was categorized for each trial based on the initial judgment of hand position and the maximum change in perceived hand position between consecutive judgments. If the initial hand position judgment was closer to the reflection hand than to the actual hand (i.e., greater than 8 cm), then the trial was categorized as an Immediate experience of the illusion. If the perceived hand position shifted by less than 8 cm throughout the trial, then the trial was categorized as No Illusion. For the 30 cm Distance condition of Experiment 2, the cutoff value for Immediate and No Illusion trials was scaled in proportion to the greater absolute illusion strength of the 30 cm compared to the 15 cm condition. This scaling factor was also used for Experiment 3, where all trials were at a 30 cm distance. Among the remaining non-Immediate trials where the illusion was experienced, if the largest change in consecutive judgments throughout a trial was no more than 40% of the total shift from the initial judgment to the most illusory judgment (i.e., greatest proprioceptive drift), then the trial was categorized as showing a Gradual illusion trajectory. If the largest change in consecutive judgments throughout a trial was greater than 65% of the total shift from the initial judgment to the most illusory judgment, then the trial was categorized as showing an Abrupt illusion trajectory. If the largest change in consecutive judgments throughout a trial was intermediate between these cutoff values, then the trial was categorized as showing an Intermediate illusion trajectory. Because data was only collected for two time points in the Infrequent condition of Experiment 1, the Infrequent trials were not categorized.

To test the construct validity of our trajectory categorization scheme, we trained a *k*-nearest neighbors classifier to predict trajectory category from the 13-dimensional vector of hand position judgments for each trial. *k* values were selected by averaging values selected by internal tuning across 50 independent resampling iterations; optimal *k* values ranged from 5 to 11. We used repeated stratified cross-validation with 5 stratified folds X 10 repeats. Reported classification rates are the mean cross-validated accuracies across folds and repeats. To test whether the classification rates yielded by this analysis performed better than chance, we used permutation testing, performing the entire *k*-nearest neighbors algorithm on 1,000 permutations in which the class labels were randomly shuffled. The proportion of permutations in which the classification rate of the permutation exceeds or equals the classification rate for the actual, non-shuffled dataset is the *p* value for the permutation test. The analysis yielded correct classification rates of 73.49% for Experiment 1, 79.05% for Experiment 2, 84.94% for Experiment 3, and 84.36% for Experiment 4, all $p < 0.001$. Because the Abrupt, Intermediate, and Gradual trials exist on a continuum, we were curious how well these trials could be differentiated amongst themselves. In restricted datasets excluding the Immediate and No Illusion trials, correct classification rates were 73.01 for Experiment 1, 46.49% for Experiment 2, 66.12% for Experiment 3, and 65.81% for Experiment 4, all $p < 0.001$, indicating that even the trajectory types that exist along a continuum are reasonably differentiable from each other.

Binomial mixed models

To examine the effects of our experimental manipulations on the frequency of the different illusion trajectory categories, we ran binomial general linear mixed effects models using the lme4 R package. For each experiment, the principal experimental manipulations were modeled as fixed effects (Movement Synchrony for Experiment 1, Distance and Movement Synchrony for Experiment 2, Rate of Tapping and Movement Synchrony for Experiment 3, Angular Disparity and Biomechanical Constraint for Experiment 4), and Subject was modeled as a random effect. Because the effect of these manipulations was tested on each trajectory type, statistical significance was corrected for multiple comparisons using the Benjamini-Hochberg procedure.

Tests for individual differences

We conducted two tests to determine whether trajectories of proprioceptive drift differed across individuals. The first test used the trajectory category labels described above. For each experiment, we ran 10,000 Monte Carlo simulations in which trajectory labels were randomly assigned to simulated trials and subjects in proportion to the frequency of each trajectory type in that experiment. The variance of the number of each trajectory type's count across subjects was used as a measure of how evenly that trajectory type was distributed across subjects: low variance indicates an even distribution (and less individual variation), while high variance indicates an uneven distribution (and more individual variation). The *p*-value was the proportion of simulations in which the simulated variance was higher than the observed variance. These *p*-values were corrected for multiple comparisons using the Benjamini-Hochberg procedure.

Our second test for individual differences did not rely on the trajectory category types. This analysis used the Mahalanobis distance between trials in the 13-dimensional space described by the 13 judgments of hand position for each trial. For each experiment, we compared distances for all pairs of trials within subjects to distances for all pairs of trials between subjects. A permutation-based *t*-test was used to assess significance. Determining the *p*-value through permutation testing rather than through a standard t-distribution is more appropriate in this case because a standard t-distribution assumes independence, whereas in this case each trial contributes to many trial pairs such that a standard *t*-test would overestimate the degrees of freedom. The permutation test shuffled subject labels across 1,000 permutations. The p value was the proportion of permutations in which the difference between within- and between-participant pairs was larger than the observed difference.

Decision strategy simulations

To visualize what sorts of trajectories of multisensory integration would result from the use of different decision strategies, we ran simulated trials under the assumptions of model averaging, model selection, and probability matching. The average of 1,000 simulated trials using each decision strategy were used to create representative illusion trajectories for each decision strategy. In each simulated trial, *p(common)* was modeled as a logistic growth curve. The supremum of the logistic curve was drawn from a uniform distribution ranging from 0.6 to 0.9, while the curve's growth rate was drawn from a normal distribution with mean of 0.15 and standard deviation of 0.075, with a minimum acceptable value of 0.05. The logistic curve was centered at 5. At each time point in the trial, a visual estimate of hand position and a proprioceptive estimate of hand position were generated. These values were drawn from normal distributions centered respectively at 6 (corresponding to the position of the reflection hand) and 0 (corresponding to the position of the actual hidden hand). The standard deviations of these distributions were held constant throughout each simulated trial. The standard deviation of the visual estimate was drawn from a normal distribution with mean of 0.05 and standard deviation of 0.025. The standard deviation of the proprioceptive estimate was drawn from a normal distribution with mean of 0.5 and standard deviation of 0.25. The maximum likelihood estimate was calculated by combining the proprioceptive and visual estimates weighted in proportion to their reliability (i.e., their standard deviations). In simulated trials using model averaging, the overall judgment at each timepoint was calculated as the weighted sum of *p(common)**(maximum likelihood estimate)+p(¬common)*(proprioceptive estimate). In simulated trials using model selection, the overall judgment at each timepoint was taken to be equal to the proprioceptive judgment when *p(common)* was less than 0.5, and was taken to be equal to the maximum likelihood estimate when *p(common)* was greater than or equal to 0.5. In simulated trials using probability matching, a decision to use either the proprioceptive estimate or the maximum likelihood estimate was made at the trial's beginning and maintained throughout the trial. The proprioceptive estimate was selected with frequency equal to *p(¬common)* at the start of the trial, and the maximum likelihood was selected with frequency equal to *p(common)* at the start of the trial.

Subject exclusion

For the ANOVAs comparing illusion strength across conditions, the binomial mixed model analyses, and the distribution of trajectory types by experimental condition, we excluded data from participants who never once experienced the illusion. Additionally, a subject who only completed 3 trials was excluded from Experiment 4. This resulted in the exclusion of 4/43 participants from Experiment 1, 8/34 participants from Experiment 2, 1/39 participants from Experiment 3, and 6/64 participants from Experiment 4. Inclusion of these participants would have changed the significance of almost none of the results (see Table S4).